Available online at www.sciencedirect.com

SciVerse ScienceDirect

Ceramics International 39 (2013) 8499–8502

CERAMICS INTERNATIONAL

www.elsevier.com/locate/ceramint

Short communication

# Monophasic $ZnFe_2O_4$ synthesis from a xerogel layer by auto combustion

A. Sutka[a,*], G. Mezinskis[a], M. Zamovskis[a], D. Jakovlevs[b], I. Pavlovska[a]

[a]*Institute of Silicate Materials, Riga Technical University, Azenes 14/24, Riga, LV-1048, Latvia*
[b]*Riga Biomaterials Innovation and Development Centre, Riga Technical University, Riga, Latvia*

Received 9 January 2013; received in revised form 25 February 2013; accepted 27 February 2013
Available online 7 March 2013

**Abstract**

The influence of sol–gel auto combustion synthesis conditions on the phase purity and microstructure of $ZnFe_2O_4$ ($ZnO \cdot Fe_2O_3$) nanopowders was studied. The phase composition was determined by X-ray diffraction and the particle size measured by scanning electron microscopy. It was found that the external conditions of the auto-combustion reaction affect the phase purity of the synthesized material. Combustion of a xerogel layer on a hot plate forms monophasic spinel zinc ferrite with a particle size ~20 nm. Practical use of synthesized $ZnFe_2O_4$ nanopowders as gas sensors with reversible response–recovery behavior to ethanol is demonstrated.


*Keywords:* Zinc ferrite; Sol–gel; Gas sensor

## 1. Introduction

Recently a considerable amount of research on nanostructured ferrites synthesized by sol–gel auto combustion methods has been carried out [1,2]. This method is quite simple and involves the formation of solution from raw materials, followed by solution evaporation and drying to obtain a xerogel, and finally auto-combustion initiated by heating above 200 °C. Phase purity, grain size and agglomeration, as well as the point defect concentration of the synthesized spinel ferrites depends on the temperature, rate and duration of the combustion reaction [3]. These parameters can be influenced by the chemical nature of the raw materials (typically metal nitrates as the cation source and citric acid, glycine or urea as the complexant), the ratio between complexant and nitrates [4], the pH value of the solution [5], chemical additives and atmosphere [6,7]. Generally, to obtain small particles and soft particle agglomerates, the combustion temperature should be low and the reaction—fast [8]. In contrast, high temperature, long reaction time and, most important, the presence of oxygen are necessary for crystallization and phase purity [8]. To obtain monophasic defect free materials, the reaction should be performed in an oxygen rich atmosphere. It is essential to vary the reaction conditions so as to increase oxygen transport in the reaction environment. From this observation the idea was born to perform the combustion reaction of thick xerogel layers in open-air atmosphere. The present investigation shows three different examples of the combustion process and its influence on particle size and phase purity of the $ZnFe_2O_4$ spinel ferrite. It was found that the phase purity of the obtained spinel ferrite differs greatly even if the combustion reaction is performed in environmental air versus a muffle oven. Practical use of the obtained nanopowders as gas sensors is demonstrated as well. Zinc ferrite has already previously been reported as a promising material for gas sensing [9]. The elaboration of easy to produce materials with improved gas sensing characteristics is a key challenge for science and industry.

## 2. Experimental details

The sol–gel auto combustion method has been used to synthesize $ZnFe_2O_4$. The materials used were iron nitrate ($Fe(NO_3)_3 \cdot H_2O$), zinc nitrate ($Zn(NO_3)_2 \cdot H_2O$) and citric acid ($C_6H_8O_7 \cdot H_2O$). The iron and zinc nitrates were dissolved in distilled water in a stoichiometric ratio. Then the reductant

*Corresponding author. Tel.: +371 26 138155.
*E-mail address:* andris.sutka@rtu.lv (A. Sutka).

0272-8842/$ - see front matter © 2013 Elsevier Ltd and Techna Group S.r.l. All rights reserved.
http://dx.doi.org/10.1016/j.ceramint.2013.02.092

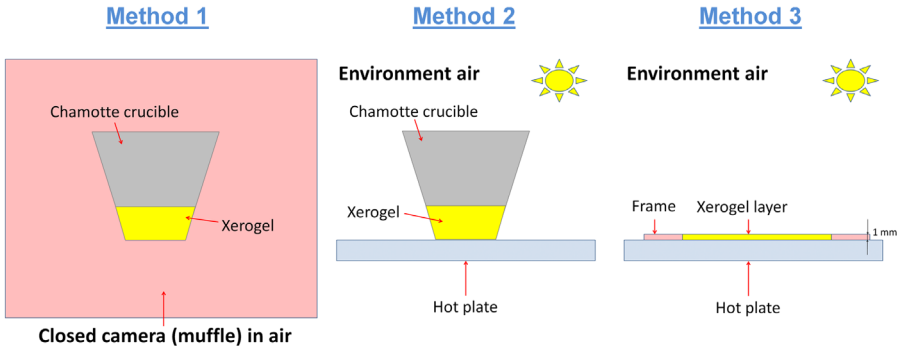


Fig. 1. Three external conditions of heating for combustion reaction initiation: Method 1—xerogel in chamotte crucible and muffle oven; Method 2—xerogel in chamotte crucible and open air; Method 3—xerogel in the form of a thick layer (1 mm) in open air.

citric acid monohydrate ($C_6H_8O_7 \cdot H_2O$) was added to the nitrate solution. The molar ratio of nitrates to citric acid was 1:1. The pH of the solution was adjusted to 7 by adding ammonium hydroxide ($NH_4OH$). The obtained mixture was evaporated continuously at 80 °C by stirring until a highly viscous gel was formed. After evaporation, the gel was left in a chamotte crucible ("Method 1" and "Method 2") or transferred in the form of a 1 mm thick layer ("Method 3") as shown in Fig. 1.

The obtained powders were characterized with an Ultima+ X-Ray diffractometer (Rigaku, Japan) with CuKα radiation. The average crystallite size $D$ was calculated using the Scherrer equation. The lattice constant $a$ was calculated from the position of the peaks using the Nelson-Riley function. Microstructural features of the powder samples were detected by SEM using a Field Emission Gun SEM (Tescan Mira/Lmu, Czech Republic).

For practical applications the gas sensing properties of $ZnFe_2O_4$ nanopowders were studied by measuring the change in DC resistivity during exposure to 100 ppm ethanol vapor in ambient air. The gas response ($S$) for the samples was calculated from the equation: $S=(R_a-R_g)/R_g$, where $R_g$ is sample resistance in the presence of ethanol vapor but $R_a$ is sample resistance in air. The lab-made experimental set-up consisted of a gas chamber—a plastic box with a hermetic lid. A custom made air lock with a sample holder and necessary electrical connections mounted into the lid was used for easy sample replacement. The sensor element was made from a ceramic alumina tube assembled with platinum wire electrodes for electrical contacts, a heater fixed inside the tube and a chromel–alumel thermocouple for temperature control. The ferrite layer on the alumina tube was deposited by a dip coating process, inserting the sensor tube into an ethylene glycol dispersion with $ZnFe_2O_4$ ferrite powder (10 wt%) at a controlled speed of 200 mm/min.

## 3. Results and discussion

Fig. 2 shows X-ray diffraction patterns of the $ZnFe_2O_4$ powders obtained with the different heating methods. A zinc oxide (ICDD 04–009-7657) impurity was identified if the

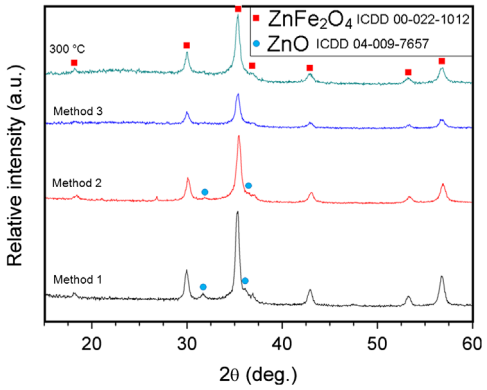


Fig. 2. XRD patterns of the $ZnFe_2O_4$ nanopowders obtained under three different auto-combustion heating conditions and the nanopowder obtained by "Method 3" annealed at 300 °C.

combustion reaction was performed in a muffle furnace or closed chamber (Method 1), as well as in a crucible in open air (Method 2). "Method 2" provided powders with a smaller content of impurities than "Method 1". If combustion of the xerogel layer on a hot plate was performed in open air (Method 3) no impurity phases were found. To verify there were no ZnO impurities in the amorphous form, powders obtained from the xerogel layers were heated to 300 °C for 3 h. As can be seen from Fig. 2, no additional peaks appear after heating; thus, it can be concluded that well-crystallized monophasic $ZnFe_2O_4$ spinel ferrite (ICDD 00-022-1012) powders can be obtained after combustion of a xerogel layer in open air. This is due to the increased oxygen transport in the reaction environment for combustion when the reaction is performed in open air. The presence of impurity phases in powders derived by "Method 1" and "Method 2" can be attributed to the decreased oxygen content inside the reaction environment, either the muffle or bulk xerogel. Oxygen accelerates the combustion process, as well as improving the crystallization of metal ions into the cubic spinel structure. The average crystallite size of the $ZnFe_2O_4$ derived using "Method 3" was 17 nm.

It was found that structural parameters of the $ZnFe_2O_4$ nanoparticles obtained by "Method 3" were unstable when heated. Crystallite size, lattice constant and degree of

Table 1
Properties of non-annealed and 300 °C annealed zinc ferrite sample derived by using "Method 3".

| | $d$, nm | $a$, Å | $I_{(220)}/I_{(222)}$ | $V_1$, cm$^{-1}$ | $V_2$, cm$^{-1}$ |
|---|---|---|---|---|---|
| Non-annealed | 17 | 8.423 | 2.18 | 550 | 442 |
| 300 °C | 19 | 8.428 | 2.37 | 542 | 414 |

inversion of non-annealed and annealed (300 °C) powders obtained from a xerogel layer are shown in Table 1. After annealing, even at relatively low temperature (300 °C), crystallite size, lattice constant and degree of inversion were all changed. The lattice constant is larger for the annealed sample. The increase in the lattice parameter could be attributed to the stresses inside the non-annealed powders [10] or due to a decrease in the degree of inversion [11]. Zinc ferrite usually forms a normal spinel structure, with zinc ions in tetrahedral lattice site and iron ions in octahedral sites. An inverse spinel structure is formed in nanosized zinc ferrite, due to its relatively low synthesis temperature, which means that the divalent zinc ion is present in an octahedral lattice site. Heating causes the migration of zinc ions from octahedral sites back to tetrahedral sites, while $Fe^{3+}$ ions migrate from tetrahedral to octahedral sites. Zinc ions being larger than $Fe^{3+}$, the narrow tetrahedral sites are expanded, leading to an increase in the lattice parameter. The increase in the X-ray diffraction peak intensity ratio $I_{220}/I_{222}$ (Table 1) for the synthesized nanoparticles also shows evidence for a decrease in the degree of inversion [11]. It is known that the degree of inversion can be estimated from XRD patterns by calculating and comparing the intensity ratios of the intensities of the (220) and (222) peaks [11].

The morphology of the "Method 3" derived $ZnFe_2O_4$ nanopowder is shown in Fig. 3. SEM micrographs demonstrate that the powders consist of agglomerated nanoparticles with a size of ~20 nm. These results are in good correspondence with the calculated crystallite sizes (Table 1). There was no difference in particle size between products from auto-combustion reactions using different combustion methods.

Before measuring the gas response of the $ZnFe_2O_4$ sample, it was stabilized at 350 °C in air for 24 h. Fig. 4(a) demonstrates the gas response ($S$) of $ZnFe_2O_4$ nanopowders to 100 ppm ethanol at different temperatures. The gas response to 100 ppm ethanol attained a maximum when operating at 275 °C. When the operating temperature is raised, desorption of inactive surface hydroxyl groups and adsorption of oxygen increases for reaction with the test gas [12]. The decrease in the gas response beyond a certain temperature is attributed to a reduced adsorption ability of the test gas and desorption of active oxygen species. The response–recovery behavior at the working temperature (275 °C) of the $ZnFe_2O_4$ nanopowder gas sensor is shown in Fig. 4(b). As expected, electrical conductivity increases when 100 ppm ethanol vapor is introduced into the atmosphere, showing n-type conductivity behavior. The electrical conductivity for n-type semiconductor ferrite samples increases when a reducing gas such as ethanol reacts with oxygen species absorbed on the surface [13]. N-type conductivity in spinel zinc ferrite is

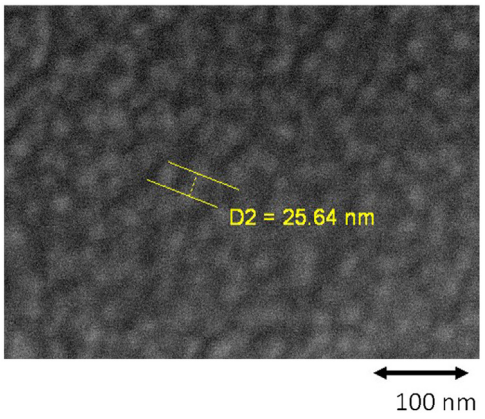


Fig. 3. SEM micrograph of $ZnFe_2O_4$ nanopowder obtained from a xerogel layer on a hot plate.

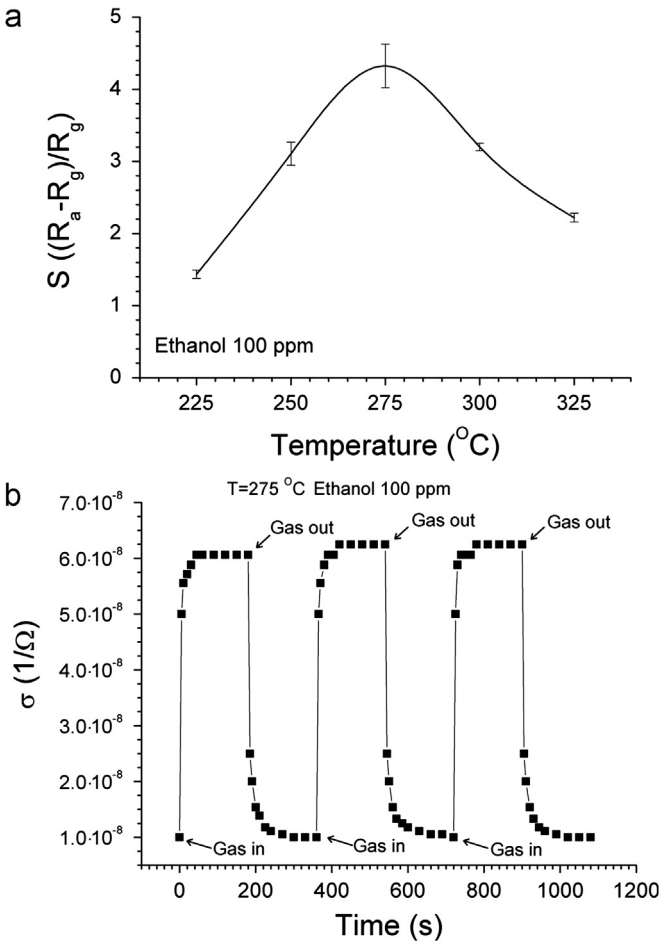


Fig. 4. Gas response (S) versus operating temperature for the 100 ppm ethanol gas for on the synthesized $ZnFe_2O_4$ nanopowder (a); electrical responses upon to ethanol (100 ppm) at the optimal operating temperature (275 °C) (b).

provided through electron hopping between $Fe^{2+}$ and $Fe^{3+}$ ion pairs located in the octahedral sites of the spinel structure [14]. When gas reacts with chemisorbed oxygen species, oxygen loss occurs, $Fe^{3+}$ reduces to $Fe^{2+}$ and conductivity increases; thus, the gas sensing mechanism is related to loss of depletive type oxygen adsorbates and, therefore, a change in material stoichiometry and electronic properties.

The response and recovery times for the tested samples (90% change in conductivity) were $<10$ s and $<40$ s, respectively. Overall, the obtained $ZnFe_2O_4$ material can be used as an effective ethanol gas sensor with fast response and recovery behavior.

## 4. Conclusions

The external conditions of the auto-combustion reaction show significant influence on the phase purity of the synthesized materials. Monophasic spinel zinc ferrite nanopowder without additional calcination was obtained after performing auto combustion of a xerogel layer on a hot plate in air. The particle size of the obtained nanopowder was $\sim$20 nm.

The synthesized $ZnFe_2O_4$ nanopowders had n-type semiconductor behavior with good response and fast response–recovery behavior in ethanol vapor. The developed technology can be used for simple, fast and cheap production of monophasic spinel ferrite nanopowders suitable for the creation of an effective gas sensor.

## Acknowledgment

The authors express their gratitude to the European Regional Development Fund for financial support within the project "Sol–gel and laser technologies for the development of nanostructures and barrier structures" Nos. 2010/0221/2DP/2.1.1.0/10/APIA/VIAA/145 and RTU PVS ID 1535.

## References

[1] S.T. Aruna, A.S. Mukasyan, Combustion synthesis and nanomaterials, Current Opinion in Solid State and Materials Science 12 (2008) 44–50.
[2] A. Sutka, G. Mezinskis, Sol–gel auto-combustion synthesis of spinel-type ferrite nanomaterials, Frontiers of Materials Science 6 (2012) 128–141.
[3] C.C. Hwang, J.S. Tsai, T.H. Huang, C.H. Peng, S.Y. Chen, Combustion synthesis of Ni–Zn ferrite powder—influence of oxygen balance value, Journal of Solid State Chemistry 178 (2005) 382–389.
[4] J. Azadmanjiri, S.A. Seyyed Ebrahimi, H.K. Salehani, Magnetic properties of nanosize $NiFe_2O_4$ particles synthesized by sol–gel auto combustion method, Ceramics International 33 (2007) 1623–1625.
[5] J. Junliang, Z. Wei, G. Cuijing, Z. Yanwei, Synthesis and magnetic properties of quasi-single domain M-type barium hexaferrite powders via sol–gel auto-combustion: effects of pH and the ratio of citric acid to metal ions (CA/M), Journal of Alloys and Compounds 479 (2009) 863–869.
[6] A.F.C.M. Costa, M.R. Morelli, R.H.G.A. Kiminami, Microstructure and magnetic properties of $Ni_{1-x}Zn_xFe_2O_4$ synthesized by combustion reaction, Journal of Materials Science 42 (2007) 779–783.
[7] L. Yu, S. Cao, Y. Liu, J. Wang, C. Jing, J. Zhang, Thermal and structural analysis on the nanocrystalline NiCuZn ferrite synthesis in different atmospheres, Journal of Magnetism and Magnetic Materials 301 (2006) 100–106.
[8] J. Qui, L. Liang, M. Gu, Nanocrystalline structure and magnetic properties of barium ferrite particles prepared via glycine as a fuel, Materials Science and Engineering A 393 (2005) 361–365.
[9] A. Sutka, J. Zavickis, G. Mezinskis, D. Jakovlevs, J. Barloti, Ethanol monitoring by $ZnFe_2O_4$ thin film obtained by spray pyrolysis, Sensors and Actuators B: Chemical 176 (2013) 330–334.
[10] A.C.F.M. Costa, A.M.D. Leite, H.S. Ferreira, R.H.G.A. Kiminami, S. Cava, L. Gama, Brown pigment of the nanopowder spinel ferrite prepared by combustion reaction, Journal of the European Ceramic Society 28 (2008) 2033–2037.
[11] M. Mozaffari, M.E. Arani, J. Amighian., The effect of cation distribution of magnetization of $ZnFe_2O_4$ nanoparticles, Journal of Magnetism and Magnetic Materials 322 (2010) 3240–3244.
[12] N. Yamazoe, J. Fuchigami, M. Kishikawa, T. Seiyama, Interactions of tin oxide surface with $O_2$, $H_2O$ and $H_2$, Surface Science 86 (1979) 335–344.
[13] P.T. Moseley, New trends and future prospects of thick- and thin-film gas sensors, Sensors and Actuators B: Chemical 3 (1991) 167–174.
[14] I.H. Gul, W. Ahmed, A. Maqsood, Electrical and magnetic characterization of nanocrystalline Ni–Zn ferrite synthesis by co-precipitation route, Journal of Magnetism and Magnetic Materials 320 (2008) 270–275.